Combustion Characteristics of a Biomass-biomass Co-combustion using Thermogravimetric Analysis

Pichet Ninduangdee*‡, Porametr Arromdee**, Arkom Palamanit***, Kittinun Boonrod****, Suriya Prasomthong*****

*Division of Mechanical Engineering, Faculty of Engineering and Industrial Technology, Phetchaburi Rajabhat University, Phetchaburi 76000, Thailand

**Department of Mechanical Engineering, Faculty of Engineering and Industrial Technology, Silpakorn University, Nakhon Pathom 73000, Thailand

***Energy Technology Program, Faculty of Engineering, Prince of Songkla University, Songkhla, 90110, Thailand

****Division of Community Development, Faculty of Humanities and Social Science, Phetchaburi Rajabhat University, Phetchaburi 76000, Thailand

*****Division of Industrial Technology, Faculty of Industrial Technology, Nakhon Phanom University, Nakhon Phanom 48000, Thailand

(ninduangdee.p@gmail, porametr@gmail.com, arkom.p@psu.ac.th, kittinun.b@gmail.com, suriya.p@npu.ac.th)

‡Corresponding Author; Pichet Ninduangdee, Phetchaburi Rajabhat University, Phetchaburi 76000, Thailand, Tel: +66 83 364 2438, ninduangdee.p@gmail.com

Received: 13.04.2022 Accepted: 18.05.2022

Abstract- The present work investigated thermal decomposition behavior of palm kernel shell (PKS), empty fruit bunch (EFB), and their blends during combustion using thermogravimetric analysis. The tests were performed for six mass proportions of PKS-EFB blends. A 15 mg biomass/blend sample was heated in a thermogravimetric analyzer at different heating rates (10, 20, 30, and 40 °C/min) and 30, 40, 50, and 60 mL/min flow rate of the furnace gas (dry air/nitrogen). Combustion characteristics: ignition and burnout temperatures, as well as a comprehensive combustion performance index of all fuel options, were determined from the TG-DTG profiles. The kinetic analysis was performed to determine the combustion kinetic parameters during (co-)combustion of the selected fuel options. The findings revealed that the combustion reactivity of EFB was higher than that of PKS, as indicated by the lower values of peak, ignition, and burnout temperatures, as well as the higher value of the comprehensive combustion performance index. The activation energy for combustion of EFB was smaller than that of PKS. With increasing EFB ratio in the fuel blends, the combustion characteristics of the fuel mixtures were improved. The activation energy for PKS-EFB co-combustion found to decrease with an increased proportion of EFB. An addition of EFB in the fuel blend can improve co-combustion reactivity, thus, enhancing fuel burnout rate, and consequently combustion efficiency of the combustion system.

Keywords Thermogravimetric study, thermal degradation, oil palm residues, co-combustion, kinetic analysis

1. Introduction

According to the recent energy and environmental crises, the development of novel energy conversion technologies from renewable resources is a challenge for the energy sector to reduce or substitute the use of fossil fuels. Among renewable resources, biomass is the one that can directly replace coal in various applications [1]. Using biomass fuels for producing thermal energy or electricity offers many

advantages compared to fossil fuels from both technological and environmental points of view [2,3].

Biomass is the main renewable energy resource in Thailand because of the agricultural foundation of this country. Sustainable agricultural biomass residues produced by the Thai agricultural sectors on a large scale can be treated as CO_2-neutral with regard to their combustion, i.e., reducing the CO_2 net emission from the domestic power generation [2]. Another apparent benefit of biomass utilization through combustion is a quite low emission of SO_2, usually due to insignificant Sulphur content in biomass [3]. Utilization of agricultural residues as energy source has gained more attention [4,5] for sustainable development and energy security of the country [6].

In 2021, Thailand produced about 3 million tons of oil palm accounted for 4 percent of the world total production [7]. During oil palm processing, a tremendous quantity of solid residues including palm kernel shell and empty fruit bunch are generated in this country, showing high potential for using as a fuel in direct combustion systems, or, alternatively, as raw material for production of biofuels. Due to a substantial availability, the energy potential of these biomasses was estimated to be about 90 PJ/year [8]. However, burning these biomasses in direct combustion systems may face some difficulties or may be not feasible, due to elevated nitrogen content in palm kernel shell as well as, very high moisture content (consequently led to quite low calorific value), and very high proportion of potassium in empty fruit bunch.

Co-firing (or co-combustion) has been proved to be one of the most effective combustion methods for resolving both operational and environmental problems of systems, due to firing the problematic fuels with high fuel-S and fuel-N, low calorific value, and consisting of low-melting ash on its own. The preferred advantages of co-firing are its flexibility with various fuel types (*i.e*., fossil fuels, biomasses, combustible waste, *etc*.) and combustion method [9,10]. Recent studies showed that co-firing of a biomass with a relatively high calorific value with another biomass with lower nitrogen and/or higher moistures contents resulted in a lowered NO_x emissions from a combustion system [11,12].

Thermogravimetric analysis (TGA) has been commonly employed for prompt investigation and comparison of the thermal and combustion reactivity of different types of solid fuels including biomass [13,14]. The TGA provides important data on devolatilization and combustion behavior, as well as on combustion characteristics, such as the ignition and burnout temperatures of biomasses, which is helpful for the prediction and interpretation of a (co-)combustion process in a real combustion system. Besides, TGA also provides the important data used to estimate combustion kinetic parameters including the activation energy, pre-exponential factor, and order of reaction. These parameters are useful for efficient design and control of thermochemical processes, as well as to build up a mathematical model describing the decomposition (or degradation) of tested material.

Numerous published studies employ TGA to assess the thermal decomposition and characteristic temperatures of combustion for different types of biomass resources [15,16]. It has been mutual agreed that the thermal degradation behavior and combustion characteristics of a lignocellulosic biomass is strongly affected by its chemical structure (hemicellulose, cellulose, and lignin). Besides, some recent published works reported studies on coal-biomass co-combustion characteristics using TGA [9,17,18]. The findings from these studies revealed that the adding biomass in the coal-biomass co-combustion led to a lowered ignition and burnout temperatures, and an increased combustion performance of the fuels. However, very limited information related to the investigation on thermogravimetric characteristics and combustion kinetics of biomass-biomass co-combustion has been reported.

This work was performed to investigate the thermogravimetric characteristics of palm kernel shell, empty fruit bunch, and their mixtures. The characteristic temperatures of combustion (*i.e*., ignition, peak, and burnout temperatures), the comprehensive combustion performance index, as well as the combustion kinetic parameters, were determined for an assessment of thermal degradation behavior and combustion reactivity of the selected fuel options. A scanning electron microscopy was also conducted to obtain the knowledge of biomass morphology used to facilitate the interpretation of the main results.

2. Methodology

2.1. Analysis of biomass properties

In the current work, the thermal degradation behavior and combustion characteristics of palm kernel shell (PKS), and empty fruit bunch (EFB), and their blends were investigated. These two residues were supplied by a local oil palm mill located in Chumporn province, Thailand. The fuel properties of both biomasses are analyzed and summarized in Table 1. The proximate analysis revealed that PKS had quite low moisture content, whereas EFB contained very high

Table 1. Fuel analysis of the selected biomasses

Biomass	Proximate analysis (wt.%, as-received basis)				Ultimate analysis (wt.%, dry ash free basis)					Chemical structure (wt.%, dry ash free basis)			LHV (kJ/kg)
	W	VM	FC	A	C	H	N	O	S	Hemicellulose	Cellulose	Lignin	
PKS	5.2	70.3	19.6	4.9	53.46	7.10	1.41	37.93	0.10	10.0	32.5	57.5	16,390
EFB	41.4	44.9	10.8	2.9	37.58	14.88	0.68	46.73	0.13	18.0	66.5	15.5	5,810

Table 2. Fuel ash analysis of the selected biomasses

Fuel ash	Composition (wt.%):									
	SiO_2	Al_2O_3	K_2O	CaO	Na_2O	MgO	Fe_2O_3	P_2O_5	SO_3	Cl
PKS	23.1	5.2	7.0	42.5	5.5	3.0	1.3	8.5	2.4	0.7
EFB	15.1	2.8	42.2	19.5	–	4.2	3.4	5.3	2.5	3.7

moisture. Volatile matter in PKS was substantial, while it was elevated in EFB. Both fuel contained quite low proportion of fixed carbon. The two biomasses had quite low content of ash. Due to substantial moisture content and low fixed carbon in EFB, this biomass fuel had a very low LHV of 5,810 kJ/kg, while PKS with lower moisture had elevated LHV of 16,390 kJ/kg. From the ultimate analysis, PKS had substantially higher nitrogen content, as compared to EFB. So, a higher NO_x emissions can be predicted when firing PKS, as compared to firing EFB using similar combustion method and condition. The analysis of chemical structure shows that lignin was the main content in PKS (57.5 wt.%), while a fibrous EFB mainly contained cellulose (66.5 wt.%).

Table 2 presents the fuel ash analysis of the selected biomasses. The analysis revealed that EFB contained a significant amount of K_2O (42.2 wt.%) and Cl (3.7 wt.%), indicating a potential risk of ash–related issues likely take place when firing this biomass in a combustion system.

Due to the high fuel-N in PKS, high moisture content in EFB (resulting in very low calorific value), and substantial amount of potassium in EFB, it is therefore reasonable to co-combust PKS with EFB to improve combustion performance and mitigate combustion–related problems likely take place during energy conversion of PKS and EFB.

2.2. Method for investigation of biomass morphology

The morphological characteristic of the selected biomasses were examined by means of a scanning electron microscope (SEM, JEOL JSM-6400). The SEM analysis was performed on the cross section of the selected fuel sample at 1000× magnification. An individual biomass sample was prepared by surface cutting, and then it was coated with a thin gold layer for electrical conductivity of the specimens.

2.3. Thermogravimetric study

Thermal decomposition behavior during (co-) combustion of the selected biomasses was investigated using a TGA–DSC1, METTLER TOLEDO thermogravimetric analyzer. All experiments were conducted beginning at 30°C through to 900°C under dynamic condition. Dry air was supplied into the TGA furnace to provide combustion environment. The (co-)combustion experiments were performed at four values of heating rate (10, 20, 30, and 40 °C/min) and flow rate of dry air (30, 40, 50 and 60 mL/min) with the aim to investigate effects of these operating parameters on the thermal and combustion characteristics of the selected fuel option. To avoid effects of heat transfer during TGA test, ground PKS and EFB with a particle size of 100–150 μm were used in all experiments. The ground biomasses were well mixed to obtain a PKS–EFB blend with different mass proportions: 100%PKS, 85%PKS+15%EFB, 70%PKS+30%EFB, 55%PKS+45%EFB, 40%PKS+60%EFB, and 100%EFB.

About 15 mg of sample was used in each experiment. The thermal event of the selected fuel option during (co-)combustion was plotted and represented by the thermogravimetric (TG) curve showing the sample mass loss and derivative thermogravimetric (DTG) curve showing the rate of mass loss. The characteristic combustion temperatures including ignition (T_{ig}) and burnout (T_b) were obtained following the related literatures [15,19]. Note that in the trials with pure biomass, nitrogen gas (N_2) was also used as a furnace medium with the aim to investigate thermal degradation during pyrolysis of both biomasses. For a given fuel option and operating condition, a triplicate testing was performed to ensure reproducibility of the finding, and it was found to be very good.

The combustion performance of individual biomass and fuel blend was evaluated by a comprehensive combustion performance index (S). The S index is related to the ignition (T_{ig}) and burnout (T_b) temperatures, as well as the maximum (DTG_{max}) and average (DTG_{mean}) weight loss rate, which can be obtained from the combined analysis of TG and DTG curves. The higher value of the S index indicates higher combustion performance and faster burnout of the feedstock. It was determined as follows [20]:

$$S = \mathrm{DTG}_{\max} \cdot \mathrm{DTG}_{\mathrm{mean}} / (T_{\mathrm{ig}}{}^{2} \cdot T_{\mathrm{b}}) \tag{1}$$

2.4. Kinetic analysis

The Coats and Redfern method [21] was employed for determination of the activation energy (E, kJ/mol), pre-exponential factor (A, 1/min), and reaction order (n), during individual combustion of PKS and EFB and their co-combustion in the thermogravimetric instrument.

Basically, the combustion process is based on the Arrhenius law, and the kinetic of reactions are follows:

$$\frac{\mathrm{d}\alpha}{\mathrm{d}t} = k(T)\, f(\alpha) = A \exp\left(-\frac{E}{RT}\right) f(\alpha) \tag{2}$$

where $k(T)$ is the combustion rate constant, $f(\alpha)$ is the reaction model, R is the universal gas constant (8.314 J/mol·K), and T is the Kelvin temperature (K).

The mass conversion ratio (α) is defined as follows:

$$\alpha = \frac{m_0 - m_\tau}{m_0 - m_{\mathrm{f}}} \tag{3}$$

where m_0, m_τ, and m_f is the initial, current, and final mass of a sample, respectively.

For the non-isothermal thermogravimetric experiment at a constant heating rate (*i.e.*, $\beta = dT/dt$), the kinetic equation can be written as:

$$\frac{\mathrm{d}\alpha}{\mathrm{d}t} = \frac{A}{\beta}\exp\left(-\frac{E}{RT}\right)(1-\alpha)^n \tag{4}$$

Following the Coats and Redfern method, Eq. (4) is integrated to be as:

$$\text{for } n=1: \quad -\ln\left[-\frac{\ln(1-\alpha)}{T^2}\right] = -\ln\left[\frac{AR}{\beta E}\right] + \frac{E}{RT} \tag{5}$$

$$\text{for } n\neq 1: \quad -\ln\left[\frac{1-(1-\alpha)^{1-n}}{T^2(1-n)}\right] = -\ln\left[\frac{AR}{\beta E}\right] + \frac{E}{RT} \tag{6}$$

With a proper selection value of n, the plot of Eqs. (5) and (6) against $1/T$ will give a linear line with a high correlation coefficient. The kinetic constants: E and A can be then derived from the slope and intercept of the fitted line, respectively.

3. Results and Discussion

3.1. Biomass morphology

Fig. 1 illustrates the SEM images showing the cross-sectional views of a PKS particle and that of individual EFB fiber. From the SEM micrographs, both biomasses exhibited a cellular structure. PKS was constructed from tightly packed cells of various sizes (mainly, 10–50 μm) filled with biopolymers and, thus, exhibiting a muscle-like structure, while the EFB fibers had a high-porous texture consisting of hollow cells, basically of 10–20 μm in size. Due to substantial content of cellulose (66.5 wt.%), fibrous particles of EFB were elastic and light, whereas PKS with the predominant lignin content (57 wt.%) and muscle-like structure was characterized by rather high density and hardness.

As follows from analyses of the fuel morphology and chemical structure shown in Table 1, with the hollow cell texture and higher hemicellulose and cellulose contents in the chemical structure, EFB is expected to exhibit higher thermal and combustion reactivity and faster fuel burnout compared to PKS.

3.2. Thermogravimetric characteristics of the original biomass fuels

Thermal decompositions of PKS and EFB tested individually under combustion (tested with dry air) and pyrolysis (tested with nitrogen) conditions at a constant heating rate of 20 °C/min and gas flow rate of 30 mL/min are shown on TG-DTG curves in Fig. 2. On raising the furnace temperature, the sample mass showed some decrease, mainly due to the consecutive thermal decomposition of the major components of lignocellulosic biomass. It is known that hemicellulose and cellulose decompositions usually take place in the low and quite narrow temperature range from 160 to 360 °C and 240 to 400 °C, respectively. For lignin, its decomposition occurs over a wide range of temperatures between 150 °C and 900 °C [13,14,16,22].

Under pyrolysis condition (tested with N_2), the thermal decomposition of PKS and EFB were somewhat similar, displaying three consecutive regions of thermal decomposition; (i) biomass dewatering, (ii) main devolatilization, and (iii) continuous slight devolatilization. This behavior is a typical appearance of pyrolysis for lignocellulosic materials [16,23].

For the first region (dewatering), the initial mass losses due to evaporation of fuel moisture were found to be about 5 wt.% for PKS and about 40 wt.% for EFB, correlated with the fuel moisture in Table 1. The dewatering temperatures (T_w), at which biomass moisture was completely vaporized, of both biomasses were quite close about 120 °C.

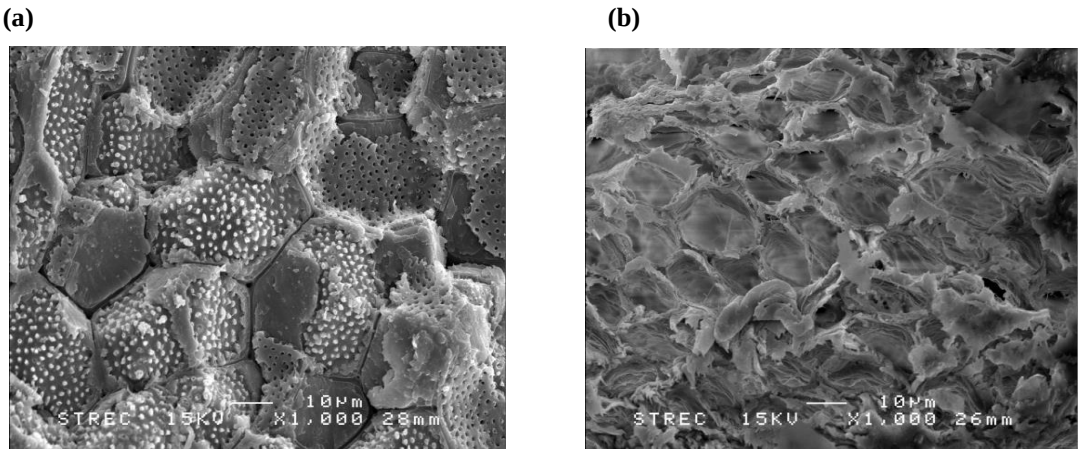

Fig. 1. SEM immages of (a) PKS and (b) EFB at 1000× magnification.

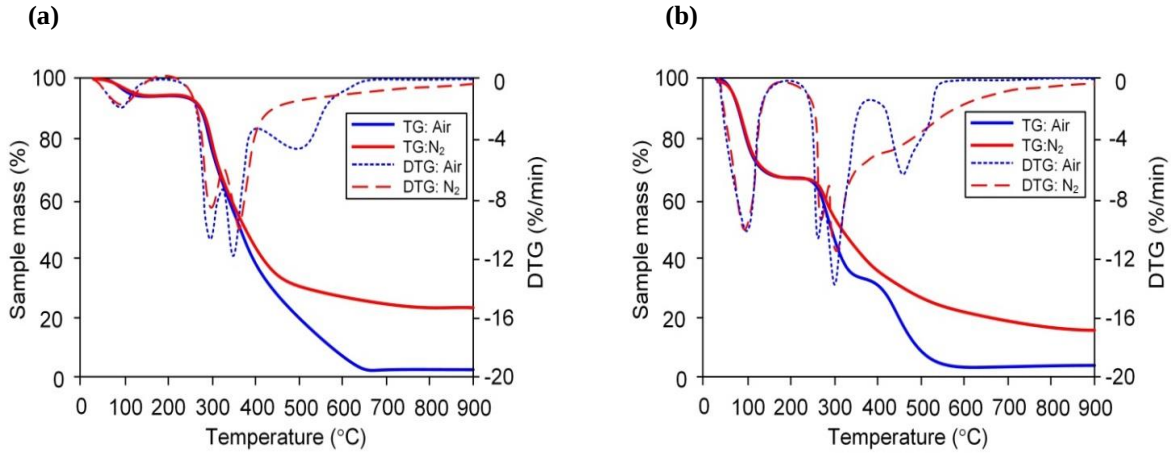

Fig. 2. TG-DTG curves of (a) PKS and (b) EFB tested individually at heating rate 20 °C/min under pyrolysis (N_2) and combustion (dry air) conditions.

From Fig. 2, the thermal decomposition of PKS and EFB mainly took place in between 190 and 410 °C. In these temperature ranges, the chemical bonds in the biomass began to break, followed by a release of the lightest volatile compounds. In this temperature region, the TG/DTG curves exhibited two peak temperatures, related to endothermic volatilization of hemicellulose, cellulose, and some part of lignin [13,14,24]. The first (T_{p1}) and second (T_{p2}) peak temperatures for PKS were found at 300°C and 350°C, whereas T_{p1} and T_{p2} for EFB were at 260°C and 302°C, respectively. From Fig. 2, the biomass degradation in this stage accounted for about 60–70% of the total weight loss.

At the temperature greater than 410 °C, one can observe a relatively low mass loss rate for both fuel options on the TG curve in Fig.2. The mass loss during this stage was mainly attributed to the decomposition of the rest lignin, accompanied by its conversion into char.

When switching furnace medium to dry air (the main experimental option of the present study), the thermal degradation behaviors of both biomass during the low temperature (below 410 °C) were quite similar to those obtained from the pyrolysis tests, showing the same number of peaks on the DTG profiles. The sample weight loss in this temperature region was related to the above-mentioned devolatilization of the high-reactive chemical constituents (hemicellulose, cellulose, and some lignin) in the biomasses [13,14,24]. Nevertheless, an oxidative environment in the TGA instrument's furnace facilitated ignition and burning of the released volatiles, consequently resulting in a greater mass reduction rate at lowered corresponding peak temperatures. Note that the first and second peak temperatures of EFB were apparently lower than that for PKS, due to a greater proportion of total hemicellulose and cellulose in EFB compared to PKS.

However, the thermal degradation of both biomasses during combustion at higher temperature region was different from those found in the pyrolysis. Another peak temperature (T_{p3}) was observed in the TG profiles at 510 °C for PKS and 470 °C for EFB. This peak temperature was mainly attributed to decomposition the rest lignin and char combustion. As seen from the DTG curve in Fig. 2, the char oxidation rate for EFB was relatively faster as compared to those for PKS. This fact can be explained by the above-mentioned hollow cell structure, as well as the lower lignin content in EFB.

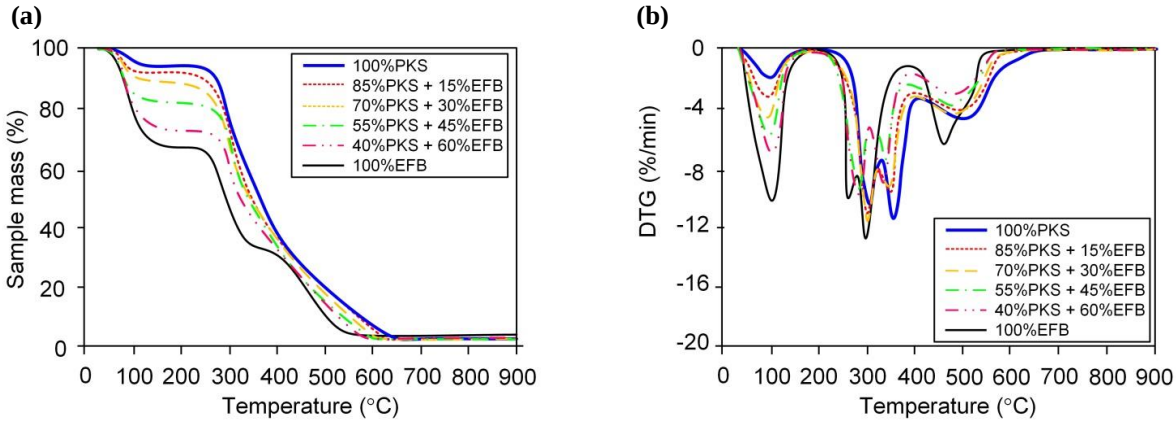

Fig. 3. The TG (a) and DTG (b) curves of PKS-EFB blends at variable proportions tested under 30 mL/min flow rate of dry air and 20 °C/min heating rate.

Table 3. Specific temperatures and comprehensive combustion performance index of PKS and EFB their blends for different fuel proportions

Sample	T_{p1} (°C)	T_{p2} (°C)	T_{p3} (°C)	T_{ig} (°C)	T_b (°C)	$S \times 10^7$ (%^{2} min^2 /°C^3)
PKS	305	357	510	275	670	5.93
85%PKS + 15%EFB	304	353	507	266	650	6.83
70%PKS + 30%EFB	302	347	504	267	625	7.61
55%PKS + 45%EFB	287	330	497	270	612	6.23
40%PKS + 60%EFB	280	325	485	270	600	6.56
EFB	270	298	470	259	575	8.42

3.3. Thermogravimetric analysis of a PKS–EFB blend

Fig. 3 shows the thermal degradation of the PKS-EFB blends, as well as those for pure PKS and EFB, during TGA experiments under dry air of 30 mL/min and 20 °C/min heating rate. It is observed from Fig. 3 that the thermal decomposition behavior during PKS-EFB co-combustion was as the results of the contribution of the individual biomass in the fuel mixture. Thus, the TG and DTG profiles of the biomass mixtures were allocated in between the ones for PKS and EFB. Three temperature regions and the corresponding peak temperatures are found on the TG and DTG profiles of the fuel mixture. As expected, the rate of demoisturizing showed an apparent increase with a greater proportion of high-moisture EFB in the fuel blend.

Table 3 summarizes the characteristic combustion temperatures and comprehensive combustion performance index of the PKS-EFB blends for different fuel proportions derived from the combined analysis of the TG and DTG curves in Fig. 3. From Table 3, the peak, ignition, and burnout temperatures of EFB were lower, whereas the value of the *S* index was higher, than that of PKS. This fact indicated a higher reactivity and burnout rate of EFB compared to PKS.

With an increased proportion of EFB in the fuel blends, all the peak temperatures were found to decrease. This effect can be elucidated by the above-mentioned higher thermal reactivity of EFB. As a result, the thermal and combustion reactivity of the PKS-EFB blend were improved. The presence of EFB decreased ignition temperature of the fuel blend. However, a further increase of EFB proportion did not impact the ignition temperature of the fuel blend significantly, as the ignition temperatures in Table 3 turned to be quite the same. This fact may be explained by an increase of moisture content in the fuel blends.

From Table 3, the presence of EFB in the fuel mixture led to a lower burnout temperature. During co-combustion of the fuel blend in the TGA system, the higher reactive biomass (EFB) with lower ignition and burnout temperature was oxidized and ignited first. The released heat from EFB combustion available in the furnace promoted ignition and combustion of the fuel blends, consequently leading to a shorter time of the fuel burnout.

In addition, the *S* index increased with increasing EFB proportion the mixture owing to a higher reactivity of this biomass, led to an improvement of ignition (T_{ig}) and burnout (T_b) characteristics of the fuel blend. However, when mixing EFB greater than 45%, the value of *S* index was found to decrease. This can be explained by an increase of moisture content in the fuel blends.

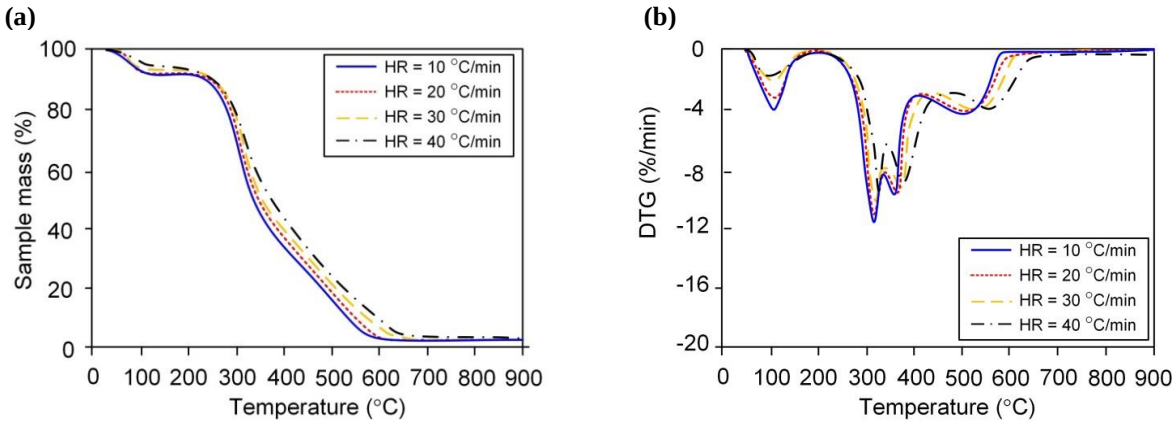

Fig. 4. The TG (a) and DTG (b) curves of a 70%PKS + 30%EFB blend tested at variable heating rates under 30 mL/min flow rate of dry air.

Based on this finding, adding empty fruit bunch to palm kernel shell can improve the combustion characteristics and reactivity, fuel burnout, and consequently combustion performance of the selected fuel.

3.4. Effects of the heating rate on thermal degradation of a PKS–EFB blend

Fig. 4 displays the effects of the heating rate on the TG and DTG curves of a 70%PKS + 30%EFB blend tested under dry air of 30 mL/min. One may observe from Fig. 4 that the heating rate exhibited some effects on both TG and DTG curves. An increased heating rate caused a shift of characteristic combustion temperatures to higher temperature regions.

When tested with lower heating rates, the samples were heated in the furnace more evenly and gradually, resulting in more effective heat transfer to the sample particle. Contrarily, an increased heating rate caused a limitation of heat transfer in the furnace leading to temperature delay between the surrounding gas and the material inside a biomass particle [25]. This phenomenon has also been observed by other studies [26,27].

3.5. Effects of the flow rate of dry air on thermal degradation of a PKS–EFB blend

Fig. 5 shows the effects of the flow rate of furnace medium on the TG and DTG curves of a 75%PKS+25%EFB mixture. The trials were performed at a fixed heating rate of 20 °C/min for variable flow rates (20, 30, 40, and 50 mL/min) of dry air. As seen in Fig. 5, the influence of this operating parameter on the thermal degradation behavior was quite insignificant, with some exemption for the lignin-related region with 400–600 °C temperatures. With a higher flow rate of dry air, the oxidation process of lignin was likely intensified, which resulted in a higher rate of lignin decomposition/char oxidation in the above-mentioned temperature region.

3.6. Combustion kinetics of PKS and EFB and their blends

Table 4 summarizes the combustion kinetic parameters: activation energy (*E*), pre-exponential factor (*A*), and order of reaction (*n*) of PKS and EFB and PKS–EFB blends, tested under dry air flow rate of 30 mL/min at 20 °C/min heating rate. These parameters were determined according to distinct temperature regimes of biomass degradation exhibited in Fig. 2. Note that the correlation coefficient, *r*, of fitting was also listed in Table 4.

Basically, the activation energy is related to the fuel reactivity: the lower activation energy means higher reactivity [28]. From Table 4, the activation energies of pure EFB obtained from all temperature ranges were apparently lower than that of pure PKS, pointing at higher reactivity of this biomass, which was consistent with the above-mentioned combustion characteristics in Table 3.

It appears that the activation energy for all temperature ranges of fuel blends slightly decreased as an increased proportion of EFB in the fuel mixtures. Therefore, adding EFB with higher reactivity in the fuel blends facilitated the combustion reaction of the PKS-EFB mixture. It can be further noticed in Table 4 that the activation energies of the selected biomasses for the stage of release and combustion of volatiles were significantly greater than those for the stage of char combustion. This fact indicates that the combustion reaction of the selected fuel option was controlled by the combustion of volatiles rather than char.

4. Conclusions

The thermogravimetric analysis (TGA) is performed to investigate thermal degradation and characteristics of the (co-)combustion of palm kernel shell and empty fruit bunch. The results show that EFB has a lower peak, ignition, and burnout temperatures, but higher comprehensive combustion performance index, as compared to PKS. This makes the combustion reactivity of EFB to be higher than that of PKS. With increasing proportion of EFB, combustion reactivity of the PKS–EFB blend has been improved, thus, enhancing fuel

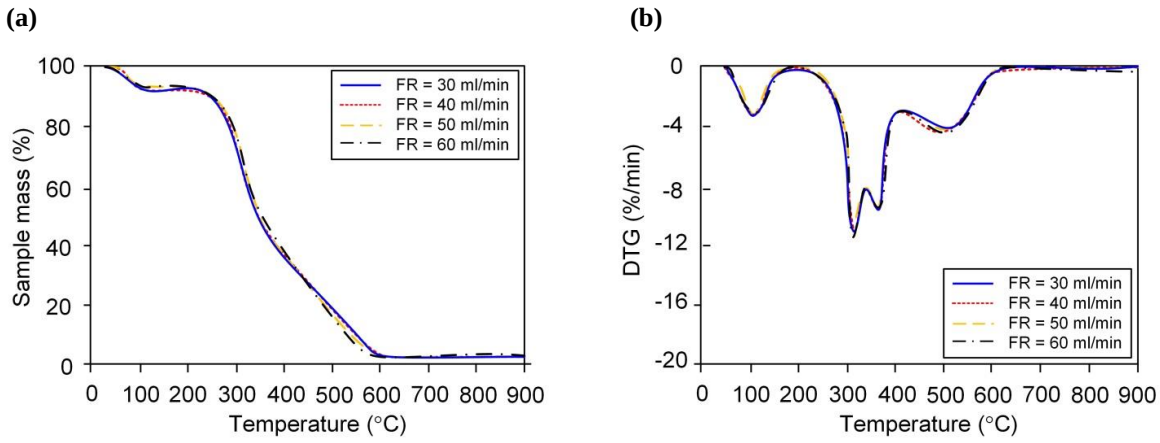

Fig. 5. The TG (a) and DTG (b) curves of a 70%PKS + 30%EFB blend tested under variable flow rates of dry air at a 20 °C/min heating rate.

Table 4. Combustion kinetic parameters of PKS and EFB and their blends for different temperature range

PKS:EFB	Temperature range (°C)	Fitting equation	*E* (kJ/mol)	A (1/min)	*n*	*r*
100:0	200–327	$y = 21.35x - 19.96$	177.5	1.992×10^{14}	5	0.9984
	327–410	$y = 9.882x - 6.57$	82.16	82.16	4	0.9931
	410–670	$y = 19.89x - 15.02$	16.54	0.012	0.6	0.9580
85:15	200–320	$y = 20.22x - 24.71$	168.1	2.180×10^{16}	5	0.9984
	320–400	$y = 8.655x - 3.770$	71.96	71.96	4	0.9833
	400–650	$y = 1.169x + 13.35$	13.46	0.051	0.6	0.9777
70:30	200–318	$y = 19.04x - 22.41$	158.3	2.050×10^{15}	5	0.9984
	318–395	$y = 8.522x - 4.969$	70.85	70.85	4	0.9914
	395–625	$y = 1.447x + 13.48$	12.03	0.033	0.6	0.9848
55:45	200–310	$y = 18.77x + 22.50$	156.0	2.231×10^{15}	5	0.9985
	310–390	$y = 6.548x + 2.163$	54.44	54.44	4	0.9956
	390–612	$y = 1.423x + 14.17$	11.83	0.015	0.6	0.9592
40:60	200–305	$y = 17.95x - 21.54$	149.3	8.132×10^{14}	5	0.9984
	305–385	$y = 6.245x - 2.444$	51.92	51.92	4	0.9931
	385–600	$y = 1010x + 12.12$	8.400	0.110	0.6	0.9833
0:100	200–274	$y = 16.88x - 17.45$	140.3	1.287×10^{13}	2.5	0.9984
	274–399	$y = 7.708x - 3.933$	64.09	64.09	4	0.9321
	399–575	$y = 3.024x + 10.17$	25.14	2.323	0.6	0.9816

burnout rate, and consequently combustion efficiency of the system. The heating rate exhibits some effects on the thermal degradation behavior of the fuel blend, while the flow rate of furnace medium shows a minor impact on the TG/DTG curves. The activation energy of EFB is lower than that of PKS. A greater ratio of EFB in the fuel mixture results in a lowered activation energy of the fuel mixture. The kinetic parameters obtained in this study can be used to predict the time-related decomposition of PKS and EFB and their blends under specified operating conditions

Acknowledgements

This work is supported by Phetchaburi Rajabhat University and the Thailand Science Research and Innovation (Project number 008-2564). Sirindhorn International Institute of Technology, Thammasat University is acknowledged for the TGA instrument. A special thank is given to Prof. Dr. Vladimir I. Kuprianov for mentorship.

References

[1] S. Naseem, M.I. Abid, M Kamran, M. R. Fazal, G. Abbas, M. R. Abid, Z. Zamir, "Rural areas interoperability framework: intelligent assessment of renewable energy security issues in Pakistan", Int. J. Smart Grid, vol. 4, pp. 43–56, June, 2020.

[2] O. Nakagoe, Y. Furukawa, S. Tanabe, Y. Sugai, and R. Narikiyo, "Hydrogen production from steam reforming of woody biomass with cobalt catalyst," 1st International Conference on Renewable Energy Research and Applications (ICRERA), Nagasaki, pp. 2–5, 11–14 November 2012.

[3] M. Telaumbanua, F.K. Wisnu, A. Haryanto, S. Suharyatun, and A. Wahyudi, "Effect of torrefaction temperature on physical properties of biopellet from variant biomass waste", Int. J. Renew. Energy Res., vol. 12, pp. 81–87, March 2022.

[4] I. Carlucci, G. Mutani, and M. Martino, "Assessment of potential energy producible from agricultural biomass in the municipalities of the Novara plain," 4th International Conference on Renewable Energy Research and Applications (ICRERA), Palermo, pp. 1394–1398, 22 - 25 November 2015.

[5] Y. Tosun, "Forestry Biomass Waste Co-Incineration in Stoker and Subsequent Solar Panel (CSP) ORC Station," 4th International Conference on Renewable Energy Research and Applications (ICRERA), Palermo, pp. 583–589, 22 -25 November 2015.

[6] L. J. R. Nunes, J. C. O. Matias, and J. P. S. Catalao, "Application of biomass for the production of energy in the Portuguese textile industry," 2nd International Conference on Renewable Energy Research and Applications (ICRERA), Madrid, pp. 336–341, 20 – 23 October 2013.

[7] Foreign Agricultural Service, U.S. Department of Agriculture, "Palm Oil Explorer" [online]. Available:

https://ipad.fas.usda.gov/cropexplorer/cropview/commodityView.aspx?cropid=4243000. [Accessed 9 March 2022].

[8] Department of Alternative Energy Development and Efficiency, Ministry of Energy, Thailand, "Thailand Alternative Energy Situation 2020", [Online]. Available: https://www.dede.go.th/download/stat63/Thailand%20Alternative%20Energy%20Situation%202020.pdf [Accessed 9 March 2022].

[9] S. Wang, C. Zou, C. Lou, H. Yang, Y. Pu, J. Luo, C. Peng, C. Wang, and Z. Li, "Influence of the synergistic effects between coal and hemicellulose/cellulose/lignin on the co-combustion of coal and lignocellulosic biomass", Fuel, vol. 311, 122585, March 2022.

[10] P. Picciano, F.X. Aguilar, D. Burtraw, and A. Mirzaee, "Environmental and socio-economic implications of woody biomass co-firing at coal-fired power plants", Resour. Energy Econ., vol. 68, 101296, May 2022.

[11] P. Ninduangdee, P. Arromdee, C. Se, and V.I. Kuprianov, "Effects of (co-)combustion techniques and operating conditions on the performance and NO emission reduction in a biomass-fueled twin-cyclone fluidized-bed combustor", Waste biomass valori., vol. 11, pp. 5375–5391, June 2020.

[12] P. Ninduangdee, and V.I. Kuprianov, "Fluidized bed co-combustion of rice husk pellets and moisturized rice husk: The effects of co-combustion methods on gaseous emissions", Biomass Bioenergy, vol. 112, pp. 73–84, May 2018.

[13] H. Haykiri-Acma, S. Yaman, and S. Kucukbayrak, "Comparison of the thermal reactivities of isolated lignin and holocellulose during pyrolysis", Fuel Process. Technol., vol. 91, pp. 759–764, July 2010.

[14] M. Varol, A. Atimtay, B. Bay, and H. Olgun, "Investigation of co-combustion characteristics of low quality lignite coals and biomass with thermogravimetric analysis", Thermochim. Acta, vol. 510, pp. 195–201, October 2010.

[15] V.I. Kuprianov, and P. Arromdee, "Combustion of peanut and tamarind shells in a conical fluidized-bed combustor: A comparative study", Bioresour. Technol., vol. 140, pp. 199–210, July 2013.

[16] S.S. Idris, N.A. Rahman, and K. Ismail, "Combustion characteristics of Malaysian oil palm biomass, sub-bituminous coal and their respective blends via thermogravimetric analysis (TGA)", Bioresour. Technol., vol. 123, pp. 581–591, November 2012.

[17] Z.B. Laougé, and H. Merdun, "Investigation of thermal behavior of pine sawdust and coal during co-pyrolysis and co-combustion", Energy, vol. 231, 120895, September 2021.

[18] C. Chen, S. Qin, F. Chen, Z. Lu, and Z. Cheng, "Co-combustion characteristics study of bagasse, coal and their blends by thermogravimetric analysis", J. Energy Inst., vol. 92, pp. 364–369, April 2019.

[19] C. Wang, F. Wang, Q. Yang, and R. Liang, "Thermogravimetric studies of the behavior of wheat straw with added coal during combustion", Biomass Bioenergy, vol. 33, pp. 50–56, January 2009.

[20] S. Niu, M. Chen, Y. Li, and F. Xue, "Evaluation on the oxy-fuel combustion behavior of dried sewage sludge", Fuel, vol. 178, pp.129–138, August 2016.

[21] A.W. Coats, and J.P. Redfern, "Kinetic parameters from thermogravimetric data", Nature, vol. 201,pp. 68–69, January 1964.

[22] H. Yang, R. Yan, H. Chen, D.H. Lee, and C. Zheng, "Characteristics of hemicellulose, cellulose and lignin pyrolysis", Fuel, vol. 86, pp. 1781–1788, August 2007.

[23] S.S. Idris, N.A. Rahman, K. Ismail, A.B. Alias, Z.A. Rashid, and M.J. Aris, "Investigation on thermochemical behaviour of low rank Malaysian coal, oil palm biomass and their blends during pyrolysis via thermogravimetric analysis (TGA)", Bioresour. Technol., vol. 101, pp. 4584–4592, June 2010.

[24] P. Kongto, A. Palamanit, P. Ninduangdee, Y. Singh, I. Chanakaewsomboon, A. Hayat, M. Wae-hayee, "Intensive exploration of the fuel characteristics of biomass and biochar from oil palm trunk and oil palm fronds for supporting increasing demand of solid biofuels in Thailand", Energy Rep., vol. 8, pp. 5640–5652, November 2022.

[25] P. Luangkiattikhun, C. Tangsathitkulchai, and M. Tangsathitkulchai, "Non-isothermal thermogravimetric analysis of oil-palm solid wastes", Bioresour. Technol., vol. 99, pp. 986–997, April 2008.

[26] S. Li, S. Xu, S. Liu, C. Yang, and Q. Lu, "Fast pyrolysis of biomass in free-fall reactor for hydrogen-rich gas", Fuel Process. Technol., vol. 85, pp. 1201–1211, July 2004

[27] J.J.M. Orfão, F.J.A. Antunes, and J.L. Figueiredo, "Pyrolysis kinetics of lignocellulosic materials—three independent reactions model", Fuel, vol. 78, pp. 349–358, February 1999.

[28] E.M.A. Edreis, G. Luo, and H. Yao, "Investigations of the structure and thermal kinetic analysis of sugarcane bagasse char during non-isothermal CO_2 gasification", J. Anal. Appl. Pyrolysis, vol. 107, pp. 107–115, May 2014.